Available online at www.sciencedirect.com
ScienceDirect
Journal of the European Ceramic Society 28 (2008) 77–83
www.elsevier.com/locate/jeurceramsoc

Young's modulus of some SOFCs materials as a function of temperature

Sophie Giraud *, Jérôme Canel

CEA-Saclay, DEN-DANS/DMN/SRMA/LTMEx, Bâtiment 460, 91191 Gif sur Yvette Cedex, France

Received 10 November 2006; received in revised form 15 May 2007; accepted 25 May 2007
Available online 13 August 2007

Abstract

Solid oxide fuel cells (SOFCs) have been under great consideration during this last decade and much effort has been dedicated to model their thermo-mechanical behavior, trying to take into account the different properties of the materials, such as their elasticity. In this paper, we report the elastic behavior of three classical materials used in SOFCs as a function of temperature: Yttria stabilized zirconia (YSZ), $La_{0.8}Sr_{0.2}MnO_3$ (LSM) and Ni-YSZ. Both YSZ and LSM present unusual behaviors. The elastic modulus of YSZ first decreases slowly up to 150 °C, then dramatically up to 550 °C (certainly due to atomic motion) and finally increases probably because of an order–disorder transition (oxygen vacancies). The state of the art on zirconia was reviewed. For the LSM material, Young's modulus could not be determined below 600 °C. Above this temperature, samples with totally closed porosity present a continuously increasing modulus, while the other samples have a quite constant modulus.

Keywords: Elastic properties; Fuel cells; ZrO_2

1. Introduction

Since the last decade, the interest concerning SOFCs has greatly increased. Despite extensive research on the materials, the most frequently used are still yttria stabilized zirconia (YSZ) for the electrolyte, Lanthanum strontium manganite (LSM) for the cathode and Ni-YSZ cermet for the anode.

The development of SOFCs requires simulation of their behavior by thermo-mechanical models, which in turn require reliable values for the thermal and mechanical properties of the materials. For instance, the elastic constants were determined for a wide range of compositions in the ZrO_2–Y_2O_3 system at room temperature.[1–5] A value of 220 GPa was given for fully dense samples of 6.5, 7.5 and 8% mol of Y_2O_3.[3–5] Young's modulus as a function of temperature has also been reported for zirconia stabilized with Y_2O_3, CaO, ….[5–9] However, much less literature is available concerning the elastic moduli of the cermet Ni-YSZ[10] and the perovskite LSM.[11]

In this paper, we report and discuss the results of the Young's modulus measurements versus temperature of the following materials: zirconia stabilized with 8% mol of Y_2O_3 (YSZ), $La_{0.8}Sr_{0.2}MnO_3$ (LSM) and a Ni-YSZ cermet. Furthermore, we present an extensive overview and discussion of the state of the art concerning YSZ.

2. Experimental

2.1. Samples preparation

The YSZ and LSM samples were prepared with commercial powders, respectively, from TOSOH (TZ-8Y) and MEDICOAT. Both powders were cold isostatically pressed at 250 MPa into, respectively, one and four cylindrical green bodies for YSZ and LSM. YSZ was sintered at 1350 °C for 3 h in air. Each one of the four LSM green bodies was heat treated in air at different temperatures in order to obtain samples of various porosities. For the cermet Ni-YSZ, a commercial anode (Indec Company) in an oxidized form NiO-YSZ (50% wt of NiO) was taken and then reduced in hydrogen.

2.2. Samples characterization

Porosity of the samples was determined by water immersion and closed porosity of YSZ was measured by He pycnome-

* Corresponding author. Tel.: +33 1 69 08 25 14; fax: +33 1 69 08 82 52.
E-mail address: sophie.giraud@cea.fr (S. Giraud).

0955-2219/$ – see front matter © 2007 Elsevier Ltd. All rights reserved.
doi:10.1016/j.jeurceramsoc.2007.05.009

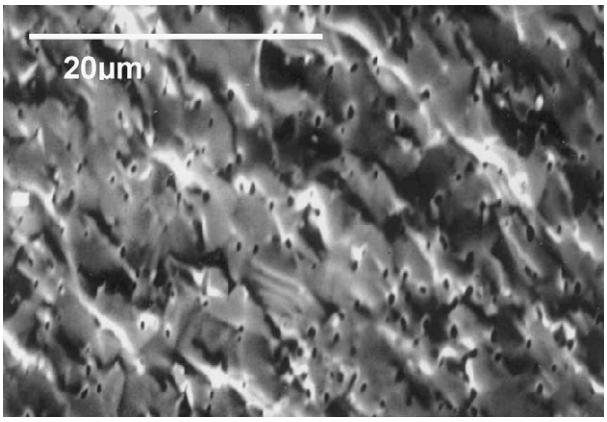

Fig. 1. Surface fracture of the YSZ sample.

try. Scanning electron microscopy was performed on fractured samples using a Stereoscan 120 to observe the different microstructures. The crystallographic phases of YSZ and LSM were checked by X-ray diffraction using, respectively, a Bruker D8 in temperature (heating and cooling) and a SIEMENS D5000 at room temperature both with a Cu Kα radiation.

Elastic modulus was determined by the impulse excitation technique (IET) using a Grindosonic (LEMMENS Company, Belgium). Torsion and flexion resonance frequencies were measured at room temperature on discs. Elastic constants (Young's modulus (E), shear modulus (G) and Poisson's ratio (ν)) were calculated assuming isotropic elasticity. The measurements versus temperature were performed under a static argon atmosphere on parallelepipedic samples. In this case, only the flexural mode can be obtained and one of the constants of elasticity (most generally ν) has to be considered constant to be able to get E and G out of the three equations defining isotropic elasticity. Therefore, in order to calculate Young's modulus, the variations of Poisson's ratio with the temperature were neglected and its value at room temperature was used.

3. Results and discussion

3.1. Zirconia stabilized with 8% mol of Y_2O_3 (YSZ)

YSZ is a material currently used as electrolyte in SOFC. In this application, it has to be as dense as possible to avoid gas leakage between anode and cathode. The sample was prepared for this purpose and its porosity evaluated by water immersion and helium pycnometry revealed only a closed porosity evaluated to $2 \pm 0.5\%$; the uncertainty is quite high. The microstructure of the sample is displayed on Fig. 1 and confirms the presence of closed pores of submicrometric size.

The phase diagram ZrO_2–Y_2O_3 is much debated. Yashima et al.[12] shows all the discrepancies encountered in the literature. He proposes a stable-metastable phase diagram for the ZrO_2 rich part. It displays the phases usually described: monoclinic, cubic and the two known tetragonal ones, but also a third tetragonal metastable phase obtained by air quenching (t″).[13] The cell's parameters of this phase are identical to those of the cubic one and the difference is due to the oxygen displacement along the c axis which is responsible for the tetragonal symmetry. Thus, if we refer to the phase diagram given by Yashima et al.,[12] the zirconia stabilized with 8% mol Y_2O_3 should not be cubic. On the other hand, Irvine et al.[14] consider that the composition $Y_{0.15}Zr_{0.85}O_{1.925}$, which corresponds to 8% mol of Y_2O_3, shows a cubic fluorite structure at a macroscopic scale containing short range order microdomains which are detected using electron diffraction. Therefore, in order to check the cubic character of our material, X-ray diffraction was performed at room temperature (Fig. 2), and also at different temperatures (Fig. 3). Note that at a given temperature, the diagrams obtained while heating and cooling are identical. If the material had contained the monoclinic phase, we should see two peaks (at 28° and 31°) on both sides of the 30° peak.[15] In the high angles region, only the 4 0 0 peak is present. If the tetragonal phases t or t′ were present, the 4 0 0 and 0 0 4 peaks should be detectable. Only the displacement of the 4 0 0 peak is observed when the temperature increases or decreases. These results indicate that the material can be considered as cubic and are in better agreement with the phase diagram given by Ruh et al.[16]

At room temperature, the values of Young's modulus (E), modulus of rigidity (G) and Poisson's ratio obtained on the YSZ sample are, respectively, 205, 78 and 0.31 GPa. The elastic modulus is in correct agreement with the values given by literature[1–5] for zirconia stabilized with various contents of Y_2O_3 (Fig. 4).

Fig. 5 displays the variation of the elastic modulus of YSZ as a function of temperature. The observed behavior is rather complicated and can be divided in three regions. From ambient temperature to around 150 °C, Young's modulus decreases first slowly, and then more strongly from 150 to 550 °C with an important dispersion of the data. Finally, it increases above 600 °C. Many authors have reported a similar behavior for zirconia stabilized with various amounts of Y_2O_3, CaO, ...[5–9] In Fig. 5, yttria stabilized zirconia with 6.5% mol[5] (data corrected from porosity) and 3% mol[6] are reported. The high temperature part of the curves depends on the Y_2O_3 content. Indeed, at high temperature, the elastic modulus decreases for 3% mol, is quite constant for 6.5% mol and increases for 8% mol.

To explain the variations of the elastic modulus with temperature, some authors have mentioned elastic anisotropy.[5,17,18]

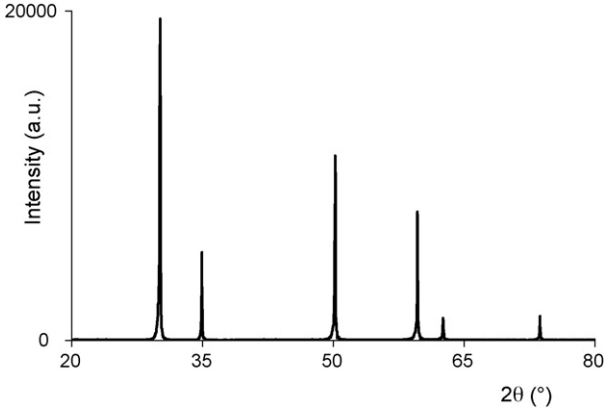

Fig. 2. X-ray diffraction pattern of YSZ at room temperature.

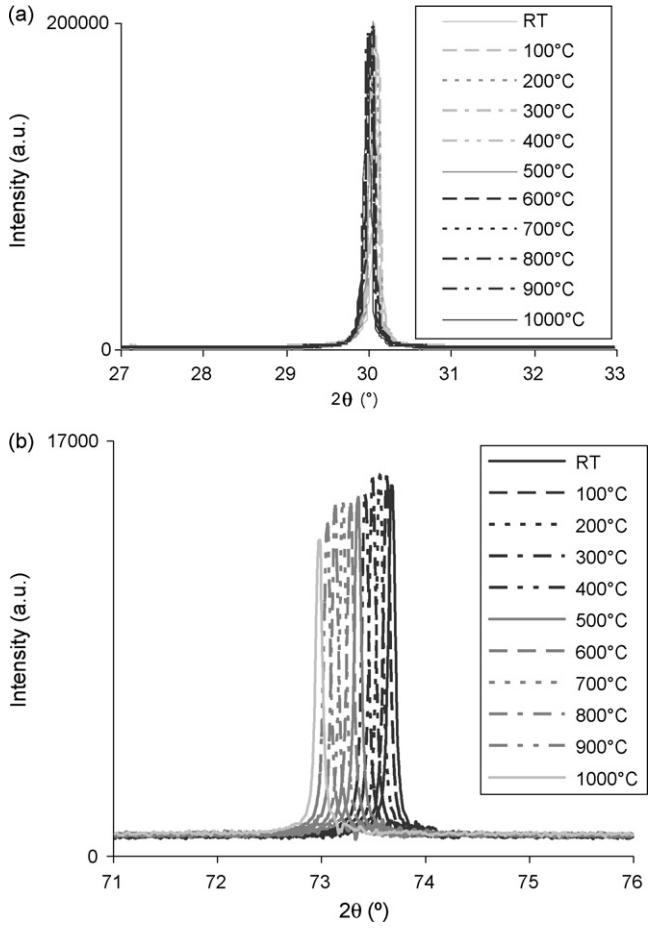

Fig. 3. X-ray diffraction pattern of YSZ as a function of temperature (a) 27°–33° and (b) 71°–76°.

On the other hand, many data on the mechanical loss are available for zirconia stabilized with various contents of Y_2O_3.[2,6,19,20] As described by Weller et al.,[19,20] the internal friction of cubic zirconia measured as a function of temperature shows a characteristic doublet peak around 130 °C but only one for the composition with 3% mol Y_2O_3. So the first and the second peaks are, respectively, assigned to the reorientation

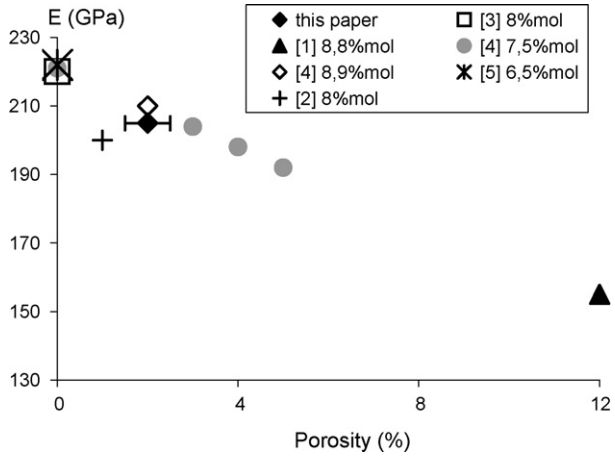

Fig. 4. Young's modulus at room temperature for zirconias stabilized with various contents of Y_2O_3.

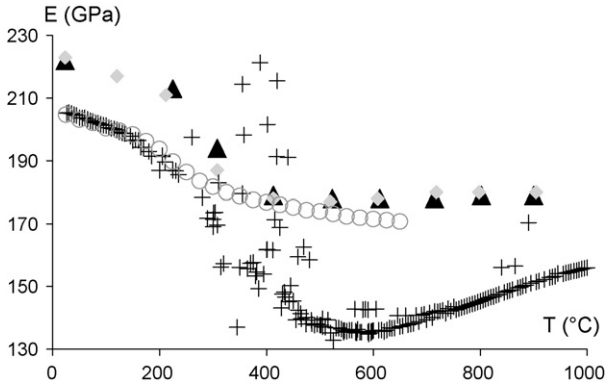

Fig. 5. Young's modulus as a function of temperature of zirconias with 8% mol (+), 6.5% mol ((▲, ◆)[5] and 3% mol (◯)[6] of Y_2O_3.

jumps of the pairs $V_o^{\bullet\bullet}$–Y_{zr}' representing the elastic and electric dipoles and to the relaxation of oxygen vacancies within a cluster of two (or more) yttrium ions.[19] This loss of energy due to the atomic motion takes place in the range of temperature corresponding to the strong decrease of YSZ Young's modulus from 150 to 550 °C and to the scattering of the values. Indeed, mechanical loss is often responsible of large scattering of the values.

Young's modulus is calculated using the following equation[21]:

$$E = 0.94642\frac{\rho l^4 \mathrm{fr}^2}{t^2} T(t, L, v)$$

fr: measured resonance frequency; v: Poisson's coefficient; L: length of the sample; t: thickness of the sample; l: width of the sample; ρ: density of the material.

Since the sample's dimensions are very important parameters, their variations (and, therefore, the thermal expansion coefficient) have to be considered. We took a constant thermal expansion coefficient over the whole range of temperature. But in the literature, a discontinuity in the thermal expansion coefficient is observed around 650 °C by Gibson and Irvine,[22] which is indicative of a second-order transition. A change in the slope of the Arrhenius plot for conduction was also reported to occur at the same temperature.[14,22,23] At higher temperature, the low temperature defect ordered structure is destroyed corresponding to the breakdown of local ordering of vacancy-dopant complexes. This order–disorder transition could explain the volume increase,[22] resulting in a higher stress level in the sample and finally in a higher Young's modulus.

3.2. $La_{0.8}Sr_{0.2}MnO_3$ (LSM)

LSM is generally used as a cathode material in SOFCs. It has to exhibit a relatively high porosity in order to allow a good circulation of gases. But since the porosity is responsible for degradation of the mechanical behavior, it was decided to perform a complete study of the mechanical properties versus temperature including some samples showing only a few percents of porosity. The porosity of all the samples was evaluated by immersion in water and the values are reported in Table 1.

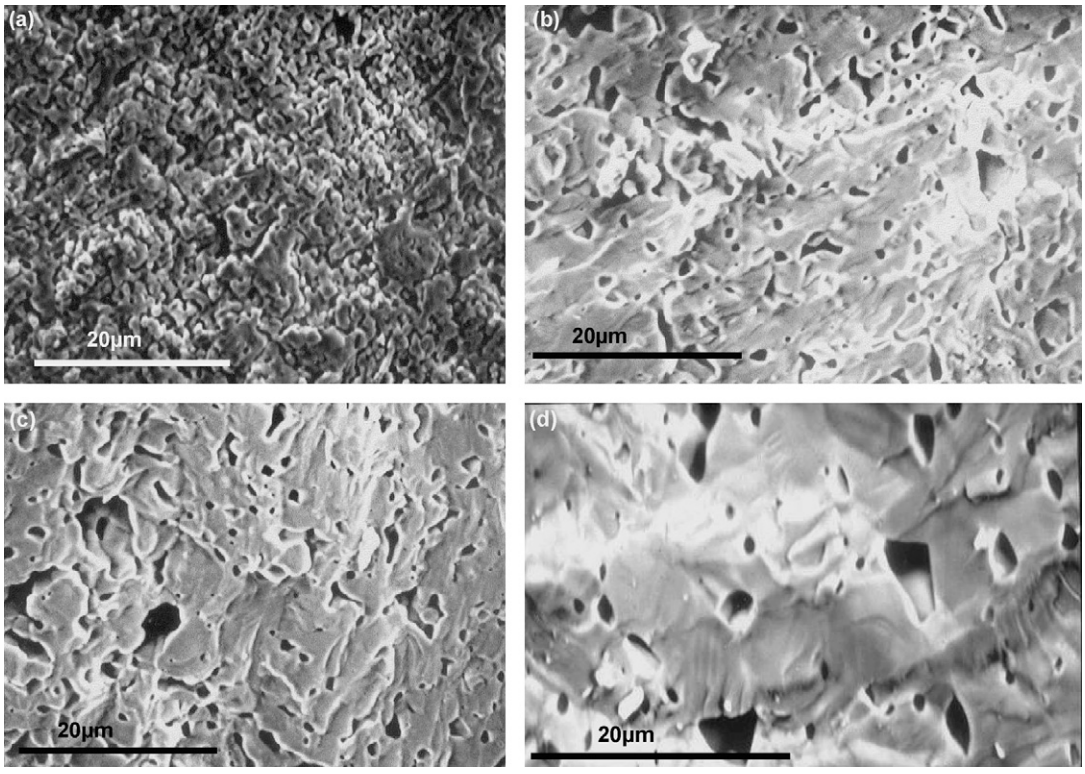

Fig. 6. Surface fracture of the LSM samples: (a) LSM-1, (b) LSM-2, (c) LSM-3 and (d) LSM-4.

The microstructures are presented in Fig. 6. They show a relatively homogeneous porosity in each sample. Porosity decreases from LSM-1 to LSM-4. Some defaults were noticed in some of the massive samples; the bars and discs were cut by avoiding them. Defaults can decrease the rigidity.

An X-ray diffraction pattern of the LSM-4 sample is displayed in Fig. 7. The peaks can be indexed in the monoclinic cell given by the JCPDS 00-040-1100 for the $La_{0.8}Sr_{0.2}MnO_3$ compound. However, it is also possible to index the diffraction lines in a rhombohedral cell.[24–26] The literature reports the existence of some phase transitions for the family of compounds $La_{1-x}Sr_xMnO_3$. A rhombohedral–cubic transition happens at a temperature which depends on the x value. For example, the transition temperature are, respectively, 1235 and 180 °C for $x = 0.2$ and 0.5.[26] Hammouche et al.[24] point out the fact that no transition should occur below a temperature of 1000 °C for $x = 0.19$; on the other hand, he does not either mention a phase transition for $x = 0.5$. So, in the temperature range explored in the present work, there is no phase transition. It is noteworthy that some insulator–metal and paramagnetic–ferromagnetic transitions were characterized around 75 °C for $x = 0.2$.[27]

The values of the elastic constants at room temperature are reported in Table 2. In order to verify the good reproducibility of the mechanical measurements, two samples were tested for each LSM materials except for LSM-2 (lack of material). The results show a good reproducibility. Fehringer et al.[11] finds a Young's modulus equal to 124 GPa, a modulus of rigidity of 46 GPa and a Poisson's ratio of 0.36 for a sample of LSM with a porosity of 2% at room temperature. These values are in good agreement with the present work.

The impact of the porosity over the elastic modulus is shown in Fig. 8 at room temperature. As expected, Young's modulus decreases when the porosity increases.

Table 1
Porosities of the various LSM samples

Sample	LSM-1	LSM-2	LSM-3	LSM-4
Open porosity (OP)%	29	9	0	0
Closed porosity (CP)%	0	2.5	9	3–4

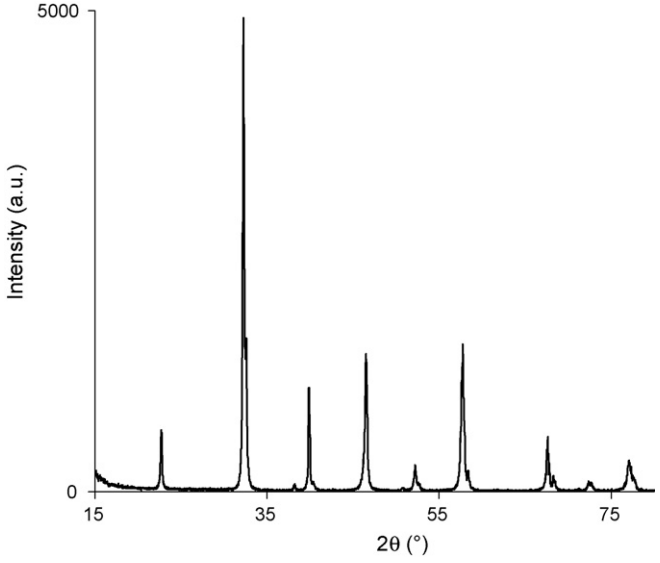

Fig. 7. X-ray diffraction pattern of LSM-4 at room temperature.

Table 2
Elastic constants at room temperature for all the LSM samples

Sample	LSM-1-a	LSM-1-b	LSM-2-a	LSM-3-a	LSM-3-b	LSM-4-a	LSM-4-b
E (GPa)	41	40	87	102	97	108	113
G (GPa)	16	16	33	38	36	40	41
ν	0.28	0.27	0.34	0.35	0.36	0.36	0.36

Samples are referenced with the number of the batch (1–4) and a letter (a, b) corresponding to different samples of the same batch.

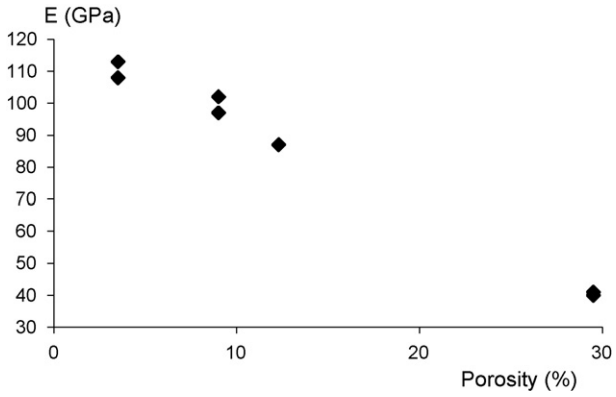

Fig. 8. Young's modulus as a function of porosity at room temperature for LSM.

The values of the elastic modulus as a function of temperature are reported in Fig. 9 for all the samples. Below a temperature ranging from 350 to 600 °C, depending on the porosity of the material, the results are strongly dispersed and were not reported in Fig. 9. This is not due to the experimental set-up, as it sometimes occurs when the vibrations frequencies are below the detectors limit, which is not the case here. Therefore, it should be due to the material's ability to absorb vibrations.

At higher temperature, the Young's modulus behaves differently depending on the kind of porosity of the samples. On one side, the samples with totally or partially opened porosity present a more or less constant elastic modulus with a good reproducibility. For LSM-1-1 and LSM-1-2, Young's modulus reaches, respectively, constant values of 48 and 51 GPa at high temperatures. These values are slightly higher than the room temperature ones. For LSM-2, elastic modulus oscillates between 103 and 106 GPa which is also higher than the ambient value.

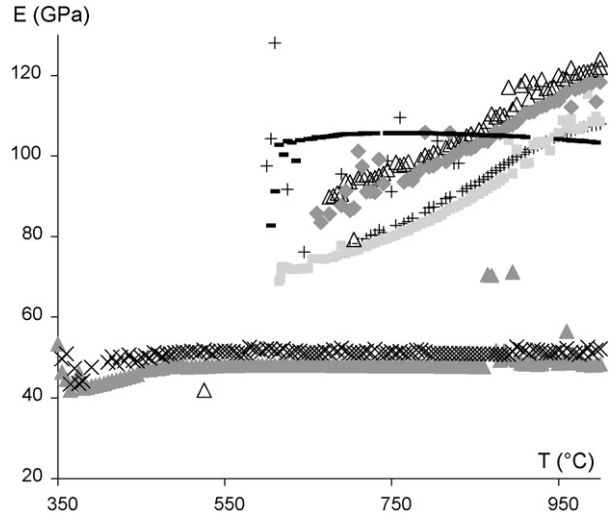

Fig. 9. Young's modulus of LSM as a function of temperature. LSM-1-1 (▲), LSM-1-2 (×), LSM-2-1 (-), LSM-3-1 (+), LSM-3-2 (■), LSM-4-1 (△), LSM-4-2 (◆).

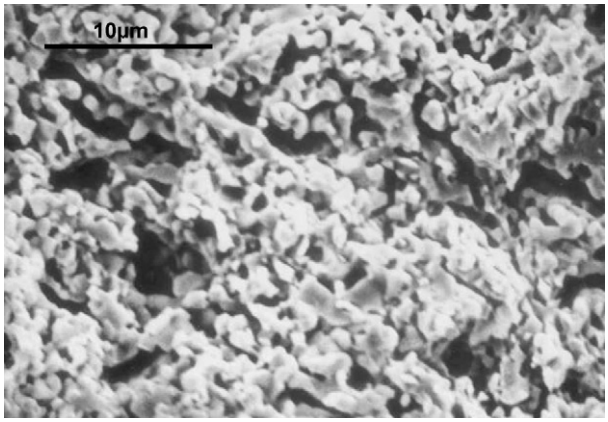

Fig. 10. Surface fracture of the Ni-YSZ sample.

On the other side, the samples with a fully closed porosity show a very different behavior. Indeed, in this case, the elastic modulus increases strongly and not linearly above 400 °C. As for the other samples of LSM, some differences of around 3 GPa are measured for samples of identical porosity. The LSM-3-2 sample, containing 9% of closed porosity, has a Young's modulus of 64 GPa at 410 °C and 109 GPa at 1000 °C. The samples with 3–4% of closed porosity present a similar behavior but due to the lowest porosity, the modulus is higher and reaches 118 GPa at 1000 °C for LSM-4-2.

The thermal expansion coefficient of $La_{1-x}Sr_xMnO_3$ with $x \geq 0.19$ increases linearly from ambient to 1000 °C[24] and cannot explain the complex behaviors of the elastic moduli.

3.3. Ni-YSZ

The Ni-YSZ cermet is a usual anode material for SOFC. As the cathode, the anode must be porous. The material used for this study is a commercial one (Indec). The porosity after reduction of NiO was evaluated by water immersion at 30%. Fig. 10 shows the microstructure of this cermet.

The resonance frequencies at room temperature could not be measured on the disc because they were out of the detection limits of the system and Poisson's coefficient could not be determined. Therefore, it was considered to be equal to 0.3 for the calculations of the Young's modulus as a function of temperature (Fig. 11). Below 80 °C, there is not scattering of the

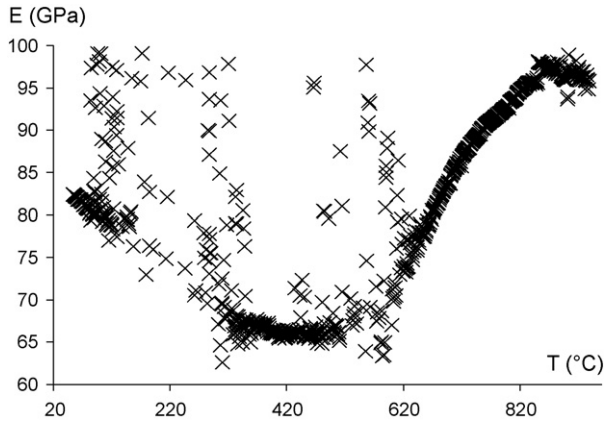

Fig. 11. Young's modulus of Ni-YSZ as a function of temperature.

measured values and so by extrapolation of the curve, the value of Young's modulus at room temperature is estimated to 85 GPa for Ni-YSZ. In the literature, Radovic and Lara-Curzio[10] report a value around 55 GPa for a cermet with 40% of porosity and containing 63% wt of NiO before reduction, which seems in accordance with our results since our sample presents a lower porosity (30%) and a lower content of NiO (50%).

Despite the fact that the experiment versus temperature was conduced under a static argon atmosphere, the sample Ni-YSZ was oxidized into NiO-YSZ. The sample was grey before measurement and green after, a color characteristic of nickel oxide NiO. This oxidation could explain the sudden increase of Young's modulus around 500 °C.

4. Conclusions

Young's modulus measurements were performed versus temperature on some well-known SOFC materials: YSZ, LSM and Ni-YSZ.

Rather complex behaviors were observed. For YSZ, the Young's modulus presents a linear decrease, but with a suddenly stronger slope beginning at 150 °C. This phenomenon is probably due to atomic motion. Then, at 600 °C, the elastic modulus increases, certainly due to an order–disorder transition.

For LSM, two different behaviors can be distinguished depending on the kind of porosity of the sample: the samples with partially or totally opened porosity present a quite constant elastic modulus while the ones with fully closed porosity present an increasing modulus versus temperature.

Concerning the cermet, we were able to get a value of the modulus estimated at room temperature using the curve of Young's modulus as a function of temperature. Unfortunately, the sample was oxidized during this measurement despite the static argon atmosphere. A new measurement should be done under a flux of argon to avoid this oxidation.

Acknowledgements

The authors gratefully acknowledge Gilles Vaux, Guillaume Loupias and Djeastri Gounassegarane for the preparation of the samples and the measurements of the elastic moduli. Thanks to Sandrine Reveillon, INSTN (France), for the easy access to the D5000 diffractometer facility.

References

1. Buckley, J. D. and Braski, D. N., Elastic modulus of stabilized zirconia. *J. Am. Ceram. Soc.*, 1967, **50**(4), 220–221.
2. Lakki, A., Herzog, R., Weller, M., Schubert, H., Reetz, C., Görke, O. *et al.*, Mechanical loss, creep, diffusion and ionic conductivity of ZrO_2-8 mol%Y_2O_3 polycrystals. *J. Eur. Ceram. Soc.*, 2000, **20**, 285–296.
3. Atkinson, A. and Selcuk, A., Mechanical behaviour of ceramic oxygen ion-conducting membranes. *S. S. I.*, 2000, **134**, 59–66.
4. Winnubst, A. J. A., Keizer, K. and Burggraaf, A. J., Mechanical properties and fracture behaviour of ZrO_2–Y_2O_3 ceramics. *J. Mater. Sci.*, 1983, **18**, 1958–1966.
5. Adams, J. W., Ruh, R. and Mazdiyasni, K. S., Young's modulus, flexural strength, and fracture of yttria-stabilized zirconia versus temperature. *J. Am. Ceram. Soc.*, 1997, **80**(4), 903–908.
6. Shimada, M., Matsushita, K., Kuratani, S., Okamoto, T., Koizumi, M., Tsukuma, K. *et al.*, Temperature dependence of Young's modulus and internal friction in alumina, silicon nitride, and partially stabilized zirconia ceramics. *Commun. Am. Ceram. Soc.*, 1984, C23–C24.
7. Sakaguchi, S., Murayama, N., Kodama, Y. and Wakai, F., The Poisson's ratio of engineering ceramics at elevated temperatures. *J. Mater. Sci. Lett.*, 1991, **10**, 282–284.
8. Wachtman, J. B. and Jam, D. G., Young's modulus of various refractory materials as a function of temperature. *J. Am. Ceram. Soc.*, 1959, **42**(5), 254–260.
9. Roebben, G., Basu, B., Vleugels, J. and Van Der Biest, O., Transformation-induced damping behaviour of Y-TZP zirconia ceramics. *J. Eur. Ceram. Soc.*, 2003, **23**, 481–489.
10. Radovic, M. and Lara-Curzio, E., Elastic properties of nickel-based anodes for solid oxide fuel cells as a function of the fraction of reduced NiO. *J. Am. Ceram. Soc.*, 2004, **87**(12), 2242–2246.
11. Fehringer, G., Janes, S., Wildersohn, M. and Clasen, R., Proton-conducting ceramics as electrode/electrolyte-materials for SOFCs: preparation, mechanical and thermal-mechanical properties of thermal sprayed coatings, material combination and stacks. *J. Eur. Ceram. Soc.*, 2004, **24**(5), 705–715.
12. Yashima, M., Kakihana, M. and Yoshimura, M., Metastable-stable phase diagrams in the zirconia-containing systems utilized in solid-oxide fuel cell application. *S. S. I.*, 1996, **86–88**, 1131–1149.
13. Yashima, M., Ohtake, K., Kakihana, M., Arashi, H. and Yoshimura, M., Determination of tetragonal-cubic phase boundary of $Zr_{1-x}R_xO_{2-x/2}$ (R = Nd, Sm, Y, Er and Yb) by Raman scattering. *J. Phys. Chem. Solids*, 1996, **57**(1), 17–24.
14. Irvine, J. T. S., Feighery, A. J., Fagg, D. P. and Garcia-Martin, S., Structural studies on the optimisation of fast oxide ion transport. *S. S. I.*, 2000, **136–137**, 879–885.
15. Ballard, J. D., Davenport, J., Lewis, C., Nelson, W., Doremus, R. H. and Schadler, L. S., Phase stability of thermal barrier coatings made from 8% wt yttria stabilized zirconia: a technical note. *J. Thermal Spray Technol.*, 2003, **12**(1), 34–37.
16. Ruh, R., Mazdiyasni, K. S., Valentine, P. G. and Bielstein, H. O., Phase relations in the system ZrO_2–Y_2O_3 at low Y_2O_3 contents. *J. Am. Ceram. Soc.*, 1984, **67**(9), 190–192.
17. Rice, R. W., Possible effects of elastic anisotropy on mechanical properties of ceramics. *J. Mater. Sci. Lett.*, 1994, **13**, 1261–1266.
18. Ingel, R. P. and Lewis, D., Elastic anisotropy in zirconia single crystals. *J. Am. Ceram. Soc.*, 1988, **71**(4), 265–271.
19. Weller, M., Herzog, R., Kilo, M., Borchardt, G., Weber, S. and Scherrer, S., Oxygen mobility in yttria-doped zirconia studied by internal friction, electrical conductivity and tracer diffusion experiments. *S. S. I.*, 2004, **175**, 409–413.
20. Weller, M., Khelfaoui, F., Kilo, M., Taylor, M. A., Argirusis, C. and Borchardt, G., Defects and phase transitions in yttria- and Scandia-doped zirconia. *S. S. I.*, 2004, **175**, 329–333.

21. Spinner, S. and Tefft, W. E., A method for determining mechanical resonance frequencies and for calculating elastic moduli from these frequencies. *ASTM Proceedings*, 1961, **61**.
22. Gibson, I. R. and Irvine, J. T. S., Study of the order–disorder transition in yttria-stabilized zirconia by neutron diffraction. *J. Mater. Sci.*, 1996, **6**(5), 895–898.
23. Vladikova, D., Kilner, J. A., Skinner, S. J., Raikova, G. and Stoynov, Z., Differential impedance analysis of single crystal and polycrystalline yttria stabilized zirconia. *Electrochim. Acta*, 2005, **51**(8–9), 1611–1621.
24. Hammouche, A., Siebert, E. and Hammou, A., Crystallographic, thermal and electrochemical properties of the system $La_{1-x}Sr_xMnO_3$ for high temperature solid electrolyte fuel cells. *Mat. Res. Bull.*, 1989, **24**, 367–380.
25. Mellergard, A., McGreevy, R. L. and Eriksson, S. G., Structural and magnetic disorder in $La_{1-x}Sr_xMnO_3$. *J. Phys.: Condens. Matter*, 2000, **12**, 4975–4991.
26. Cerva, H., Ordered La(Sr)-deficient nonstoechiometry in $La_{0.8}Sr_{0.2}MnO_3$ observed by high-resolution transmission electron microscopy. *J. Solid State Chem.*, 1995, **120**, 175–181.
27. Sotirova, E., Wang, X. L., Horvat, J., Silver, T., Konstantinov, K. and Liu, H. K., Study of structure, transport, paramagnetic and ferromagnetic properties of $La_{0.8}Sr_{0.2}Mn_{1-x}Zn_xO_3$ perovskite manganite. *Supercond. Sci. Technol.*, 2002, **15**, 346–350.